Carbohydrate Polymers 95 (2013) 1–8

Contents lists available at SciVerse ScienceDirect

Carbohydrate Polymers

journal homepage: www.elsevier.com/locate/carbpol

PEGylated starch acetate nanoparticles and its potential use for oral insulin delivery

P.F. Minimol, Willi Paul, Chandra P. Sharma*

Division of Biosurface Technology, Biomedical Technology Wing, Sree Chitra Tirunal Institute for Medical Sciences & Technology, Poojappura, Thiruvananthapuram 695012, India

ARTICLE INFO

Article history:
Received 13 December 2011
Received in revised form 6 February 2013
Accepted 13 February 2013
Available online 26 February 2013

Keywords:
Insulin delivery
Starch acetate
PEG conjugation
Self-aggregation

ABSTRACT

A novel controlled release formulation has been developed with PEGylated starch acetate nanoparticles. Biodegradable polymers, such as starch, have been studied for various pharmaceutical applications because of their biocompatibility and biodegradability. Starch acetate is one of the hydrophobic biodegradable polymers currently being used or studied for controlled drug delivery. Polyethylene glycol was conjugated with starch acetate, to obtain an amphiphilic polymeric derivative. On its incubation with insulin solution at the critical micelle concentration, self-aggregated nanoparticles with mean particle size of 32 nm are formed. These self-aggregated nanoparticles with associated insulin have enhanced encapsulation efficiency. The mean particle size of these nanoparticles increased with the increase in the molecular weight of PEG. Present study indicated that PEGylated starch acetate nanoparticles are highly bioadhesive and can be utilized as a carrier system for controlled delivery of insulin or other proteins for various therapeutic applications.

1. Introduction

Starch is one of the better known natural and biodegradable biopolymers. Starch and its derivatives received much attention in the food, plastic and pharmaceutical industries because of its gelling, film forming and biodegradable properties (Ogura, 2004). The major drawback of starch in use as a controlled release agent is its hydrophilicity (Michailova, Titeva, Kotsilkova, Krusteva & Minkov, 2001). During the last decade, new generation polymeric materials have been investigated for drug delivery applications. Different modifications or derivatization techniques have been tried for developing new polymers from natural biopolymers. One approach is acetylation of starch which converts the hydrophilic starch to hydrophobic starch acetate. Starch acetate has been widely used for drug delivery applications (Korhonen, Kanerva, Vidgren, Urtti & Ketolainen, 2004; Nutan, Soliman, Taha & Khan, 2005; Nutan, Vaithiyalingam & Khan, 2007; Pajander, Soikkeli, Korhonen, Forbes & Ketolainen, 2008; Pohja, Suihko, Vidgren, Paronen & Ketolainen, 2004; Pu, Chen, Li, Xie, Yu & Li, 2011; Tuovinen, Peltonen, et al., 2004; Tuovinen, Ruhanen, et al., 2004; van Veen et al., 2005; Xu, Yang & Yang, 2009) and has also been investigated as tissue engineered scaffold (Guan & Hanna, 2004; Reddy & Yang, 2009).

Acetylation of starch has received much attention for varied drug delivery applications, such as in the preparation of coatings for sustained release of drugs. Hydrophobically modified polymers have attracted much attention in drug delivery applications due to their subtle balance of hydrophilic–hydrophobic nature and biodegradability (Daoud-Mahammed et al., 2007; Wintgens & Amiel, 2005). They spontaneously self-associate forming hydrophobic cores with considerable potential in drug/gene delivery research and other biomedical applications (Couillet, Hughes & Maitland, 2005; Nilsson, Thuresson, Lindman & Nyström, 2000). This self-association does not allow fluids to penetrate into the particles thereby protecting the encapsulated proteins from the proteolytic enzymes in the intestine. These nanoparticles are utilized for drug delivery applications because of their high stability, prolonged residence time, high drug encapsulation, better storage life and the ability to translocate through the intestinal barrier; by the paracellular pathway or via M cells in Peyer's patches (Hussain, Jaitley & Florence, 2001). Polymeric micelles are systems constituted by self-aggregation of graft-copolymers bearing both hydrophilic and hydrophobic chains (amphiphilic polymers). In aqueous medium at a proper concentration (critical aggregation concentration, CAC) these copolymers aggregate, forming colloidal micellar systems having a hydrophobic core and a hydrophilic shell (Nagarajan, 2011). Active molecules can be either covalently or physically linked to amphiphilic copolymers, and in the aggregation process remain incorporated in the hydrophobic core. The dissociation process of these colloids and the hydrolysis of

* Corresponding author. Tel.: +91 471 2520214; fax: +91 471 2341814.
E-mail address: sharmacp@sctimst.ac.in (C.P. Sharma).

0144-8617/$ – see front matter © 2013 Elsevier Ltd. All rights reserved.
http://dx.doi.org/10.1016/j.carbpol.2013.02.021

subsequent chemical linkages allow the release of the active substances (Kim, Cha & Ahn, 2010). It is hypothesized that hydrophobic starch acetate on reaction with polyethylene glycol can self-aggregate, in the same way, to form a hydrophobic core protecting the drug inside. Therefore, an attempt has been made to develop and characterize self-aggregating nanoparticles from PEGylated starch acetate for possible approach toward orally delivering insulin.

2. Materials and methods

Starch (soluble, ACS reagent, MW 342) and *O,O′*bis(2-aminopropyl)poly(ethylene glycol) with molecular weights of 1900, 800 and 500 were obtained from Sigma Chemical Co., USA. Acetic anhydride and dicyclohexylcarbodiimide (DCC) were from Merck KGaA, Darmstadt, Germany. Insulin (human, 400 IU/ml) was a gift from USV Ltd., Mumbai, India. ZO-1 Antibody (H-300) used for the detection of ZO-1 was from Santa Cruz Biotechnology Inc., USA (sc-10804). All other chemicals and solvents used were of analytical reagent grade.

2.1. Preparation of starch acetate

Starch was allowed to react with acetic anhydride (1:4 ratio) with sodium hydroxide as a catalyst as per the reported method (Xu, Miladinov & Hanna, 2004). Briefly, 12 g of starch was suspended in 40 ml of acetic anhydride in a round bottom flask. This was allowed to react for 30 min, and 1.5 ml of 50% sodium hydroxide was added as a catalyst. The temperature was then rapidly increased to 80 °C, and maintained for 20 h, to obtain a dark brown viscous solution. The reaction was quenched by the addition of excess ice-cold water to the viscous solution. The starch acetate precipitate was collected by filtration and washed with distilled water. Washing was continued till the NaOH traces and the brown color were completely removed. This was monitored visually and by noting the pH of the washings. The white starch acetate precipitate was then dried in an oven for 24 h at 37 °C.

2.2. PEGylation of starch acetate

Starch acetate (0.5 g) was dissolved in 20 ml of acetone. 100 mg of dicyclohexylcarbodiimide (DCC) was added to this solution and allowed to react for 1 h for the activation of OH group. 0.5 g PEG dissolved in 3 ml acetone was added to the activated starch acetate solution and allowed to react for 24 h at room temperature. After 24 h, the solution was precipitated in water and washed thoroughly. These particles were dissolved in acetone and re-precipitated in water. The precipitate was freeze dried, at −40 °C, to obtain PEGylated starch acetate.

2.3. Characterization of PEGylated starch acetate

The FTIR spectra of the starch acetate and PEGylated starch acetate were obtained from Perkin–Elmer Paragon 1000 FTIR spectrometer (KBr pellets), with a resolution of 4 cm^{-1} between 500 and 4000 cm^{-1}. A ^1H NMR analysis was performed on PEGylated starch acetate in D_2O using a 500 MHz spectrometer (Bruker Avance DPX 300). Elemental (CHN) analysis of the starch acetate, activated starch acetate and PEGylated starch acetate was done using Perkin Elmer 2400 Series II CHNS/O analyzer. The particle size and zeta potential of these self-aggregated nanoparticles were analyzed by photon correlation spectroscopy and laser Doppler anemometry, respectively, with a Zetasizer, Nano ZS and the pH titrations with MPT-2 autotitrator (Malvern Instruments Limited, UK) at 25 °C.

2.4. Critical aggregation concentration (CAC) of SA-PEG nanoparticles

PEGylated starch acetate was dissolved in acetone. This solution (0.2 ml) was added to water or insulin solution, to form micelle in water or insulin solution. The measurements were made with different concentrations of PEGylated starch acetate. The intensity of scattered light was monitored using a Zetasizer, Nano ZS (Malvern Instruments).

2.5. Preparation of self-aggregated nanoparticles and association of insulin

A solution of PEGylated starch acetate in acetone with a concentration of 0.017 mg/ml was prepared. This was added to the insulin solution (400 IU/ml) to obtain insulin loaded self aggregated nanoparticles. The nanoparticle suspension was centrifuged at 9844 × *g* for 10 min, and the pellet obtained was dried in a refrigerator at 4 °C. Encapsulation efficiency and drug loading of the nanoparticles were evaluated. A known amount of drug loaded nanoparticles was incubated at 37 °C in a known amount of phosphate buffer (pH 7.4) for 24 h. This was filtered using a 0.4 micron syringe filter and the protein content estimated by Lowry's method at 750 nm using UV spectrophotometer (UV l60A, Shimadzu). Nanoparticles formed by the addition of starch acetate to insulin solution were removed by centrifugation, and the supernatant protein was analyzed for its content. The encapsulation efficiency (EE) and loading content (LC) were calculated using the following formulas.

$$EE(\%) = (C_i - C_f)/C_i \times 100$$

$$LC(IU/mg) = (C_i - C_f)/W$$

where C_i and C_f is the initial and final protein concentration respectively and W the dry weight of nanoparticles formed.

2.6. Mucoadhesiveness of PEGylated starch acetate nanoparticles

Mucoadhesion testing of the nanoparticles was carried out using a texture analyzer (TA XT plus, Stable Micro Systems, UK) with 50 N load cell equipped with a mucoadhesive holder. Nanoparticles were attached to the cylindrical probe (10 mm in diameter) by double-sided adhesive tape. Rat intestinal tissue (about 20 × 20 mm) was equilibrated for 15 min at 37 °C before placing it onto the holder stage of a mucoadhesive holder and maintained at 37 °C during the test in buffer medium. The hydrated nanoparticles attached to the probe were then moved downward to make contact with soaked tissue at a contact force of 0.05 N. This was maintained for a period of 1 s. The probe was subsequently withdrawn at a speed of 0.5 mm/s. By using the texture analyzer, the maximum force required to separate the probe from the tissue (i.e. maximum detachment force; F_{max}) could be detected directly from Texture Exponent 32 software, and the total amount of forces involved in the probe withdrawal from the tissue (work of adhesion; W_{ad}) was then calculated from the area under the force versus distance curve. These parameters were used to compare the different test conditions or formulations.

2.7. Cytotoxicity of PEGylated starch acetate nanoparticles

The *in vitro* cytotoxicity of the nanoparticles was evaluated by MTT assay (Mosmann, 1983) done on mouse fibroblast (L929) cell lines as per the directions of ISO standard (Organisation, 2009). The cells were cultured in MEM supplemented with 10% fetal bovine serum and kept at 37 °C in a humidified atmosphere of 5% CO_2. Cells

were seeded in 24 well plates at a density of 5×10^5 cells per well and incubated for 24 h. The medium was replaced with medium containing the self aggregated nanoparticles at a concentration of 2.5 mg/ml/well. The cells were then incubated for 24 h. The medium containing test material was removed, and MTT was added to the wells at a concentration of 100 μg/well and the well plates were incubated at 37 °C for 4 h. The medium was then removed; 500 μl DMSO was added and again incubated at room temperature for 15 min to dissolve the formazan crystals. The absorbance was measured using a plate reader (Finstruments Microplate Reader USA). Percentage viability was calculated from the ratio of absorbance of the test sample to the absorbance of a negative control. The cells treated with medium were used as the negative control.

2.8. In vitro insulin release study

Measurement of the release of insulin from nanoparticles was carried out in simulated gastric (SGF, pH 1.2) and intestinal (SIF, pH 6.8) fluids. SIF and SGF were prepared fresh in the laboratory with the composition as per USP without the addition of enzymes (United States Pharmacopeial Convention, 2005). 10 mg of the drug loaded nanoparticles were introduced into 5 ml of SGF and SIF, respectively in a screw-capped bottle under sterile conditions. Aliquots of 0.5 ml each were withdrawn at various time intervals (1–8 h) and the drug contents in SGF and SIF were estimated as described earlier. An equal amount of respective buffers was added in order to maintain a constant volume.

2.9. Stability and conformation of released insulin

The released insulin samples were filtered (0.22 μm; Millipore, Ireland) prior to circular dichroism (CD, for insulin conformation) and dynamic light scattering (DLS, for insulin stability) studies to remove particulate matter and possible protein aggregates. CD spectra at 25 °C were acquired using a Jasco J-810 spectropolarimeter using a 1-cm path-length quartz cell at a protein concentration of 2 mg/ml. Analysis conditions were as follows: 0.5 nm bandwidth, 10-mdeg sensitivity, 0.2-nm resolution, 2-s response, 10 nm/min scanning speed and 200–240 nm measuring range. Each spectrum is the average of at least three runs, with buffer baseline being subtracted from the average spectra. Final spectra are presented in mean residual ellipticity. Deconvolution of CD spectra was accomplished by the SELCON method (Sreerama, Venyaminov & Woody, 1999; Sreerama & Woody, 2000) using Olis GlobalWorks software (version 4.4).

2.10. Visualization of tight junctions-actin and zona occludens 1 (ZO-1)

Caco-2 cells were seeded (at 20,000 cells/well) onto four-well cell-culture plates (Nunc). The cells were maintained in an incubator at 37 °C under 5% CO_2 and used for transport experiments 6 days post-seeding (Kitchens, Kolhatkar, Swaan, Eddington & Ghandehari, 2006). Medium was replaced with HBSS transport medium, and cells were equilibrated at least for 2 h before uptake experiments. Cells were treated with 500 μl SB particles at a concentration of 10 mg/ml for 1 h. The particles were removed by washing the cells three times with PBS. The cells were fixed with 250 μl of 4% paraformaldehyde for 20 min at room temperature. Then cells were permeabilised using 0.2% Triton X-100 in blocking solution, made of 1% (w/v) bovine serum albumin (BSA) in PBS, for 20 min. The permeabilised cells were then washed twice with PBS and incubated with 250 μl of 1% BSA for 30 min.

For actin filament visualization, the blocking solution was removed, and cells were incubated with 200 μl rhodamine phalloidin solution (0.2 μg/ml) for 20 min at room temperature. After removal of rhodamine phalloidin, the cells were treated with 1% BSA as before. The cells were washed with PBS and dried overnight at 4 °C. Images were obtained using Carl Zeiss LSM Meta 510 inverted confocal laser scanning microscope (Carl Zeiss, Germany) equipped with He/Ne laser 543. The visualization of rhodamine phalloidin was done using excitation and emission wavelengths of 543 and 605 nm respectively. For ZO-1 staining, the blocking solution was removed, and cells were incubated with 200 μl of ZO-1 antibody (0.1 μg/ml) overnight at 4 °C. After removal of the ZO-1 antibodies, the cells were treated with 1% BSA as before. The blocking solution was removed, and the cells were incubated with 250 μl FITC anti-rabbit IgG for 1 h at room temperature. The cells were washed with PBS and dried overnight at 4 °C. Images were obtained using Carl Zeiss LSM Meta 510 inverted confocal laser scanning microscope (Carl Zeiss, Germany), equipped with Argon2 laser. The visualization of FITC was done using excitation and emission wavelengths of 488 and 505–530 nm, respectively.

Table 1
Elemental analysis (CHN) of starch acetate, activated starch acetate and PEGylated starch acetate.

	Carbon (%)	Hydrogen (%)	Nitrogen (%)
Starch acetate (SA)	56.1	7.1	0.15
Activated starch acetate	63.5	8.4	1.6
SA-PEG500	67.1	9.2	8.1
SA-PEG800	66.9	9.3	8.3
SA-PEG1900	66.7	9.1	8.3

3. Results and discussion

3.1. PEGylation of starch acetate

Carbodiimide is generally utilized as a carboxyl group activating agent for amide bonding with primary amines. However, as earlier reported (Chiou & Wu, 2004), activation of hydroxyl groups using carbodiimide chemistry has been utilized for the coupling of amino groups and hydroxyl groups. We performed an elemental (CHN) analysis and NMR analysis on PEGylated starch acetate to confirm the activation and coupling of amino-PEG. Elemental (CHN) analysis of the starch acetate, activated starch acetate and PEGylated starch acetate, done using a Perkin Elmer 2400 Series II CHNS/O analyzer is reported in the Table 1. The apparent increase in the percentage of carbon and nitrogen atoms with activated starch acetate indicates the activation of hydroxyl groups. The significant increase in nitrogen atoms on PEGylated starch acetate is a direct indication of the conjugation of amino-PEG. ^{1}H NMR spectra of PEGylated starch acetate is given in Fig. 1. The chemical shifts at 3.9 ppm and 5.3 ppm as shown in the ^{1}H NMR spectra are due to NH which also indicates coupling of amino-PEG.

Fig. 2 shows the FTIR spectra of starch, starch acetate and PEGylated starch acetate. The bands at 3600–3200 cm^{-1} with starch is indicative of OH which has been substantially reduced in starch acetate and PEGylated starch acetate. The appearance of the absorption band at 1749 cm^{-1} signifies the introduction of the ester carbonyl groups C=O, C—O at 1250 cm^{-1} and are indicative of the acetylation of starch. The band at 1371 cm^{-1} represents deformation of the C—H bond. The two peaks at 1240 cm^{-1} and 1040 cm^{-1} were due to the presence of C–O–C vibrations. The peak at 2117 cm^{-1} is due to the C—N bond. The bands at 2931 and 2854 cm^{-1} are attributed to the asymmetric stretching of C—H and is indicative of PEG conjugation.

3.2. Critical micelle concentration of SA-PEG nanoparticles

Critical micelle concentration of the PEGylated starch acetate derivatives were evaluated using dynamic light scattering.

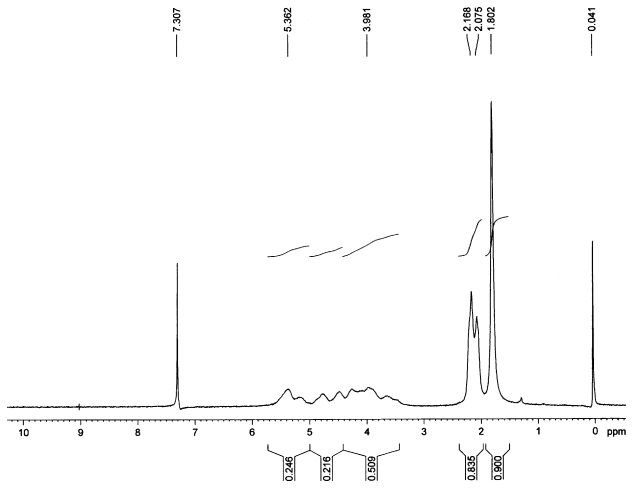

Fig. 1. ^{1}H NMR spectra of PEGylated starch acetate (SA-PEG1900).

Dynamic light scattering is an established technique for the estimation of critical micelle concentration (Pisárčik, Devínsky & Švajdlenka, 1996; Rangelov, Petrov, Berlinova & Tsvetanov, 2004). Fig. 3 is a plot of the intensity of scattered light (in kilo counts per second) as a function of the derivative concentration (mg/ml). Different concentrations of the derivatives were dissolved in acetone and were added to the buffer solution (pH 7.4). The final concentrations of the derivatives in the solution were from 0.01 mg/ml to 0.02 mg/ml. The intensity data showed that the scattering detected for derivative concentrations below the CMC were similar to that of de-ionized water. At low concentrations, the derivative molecules were unassociated, and the particle size could not be measured. As the concentration of the derivative was increased, the attractive and repulsive forces between the molecules caused self-aggregation to occur resulting in the formation of nanoparticles as the CMC was reached. The scattering intensity showed a linear increase with concentration above CMC. Thus, the intersection between the two lines at 0.015 mg/ml concentration corresponds to the CMC of PEGylated starch acetate. The CMC of the derivative with different molecular weight PEG was almost similar at 0.015 mg/ml. The average particle size of nanoparticles prepared from PEG500, PEG800 and PEG1900 were 54 ± 5 nm, 43 ± 3 nm and 32 ± 2 nm,

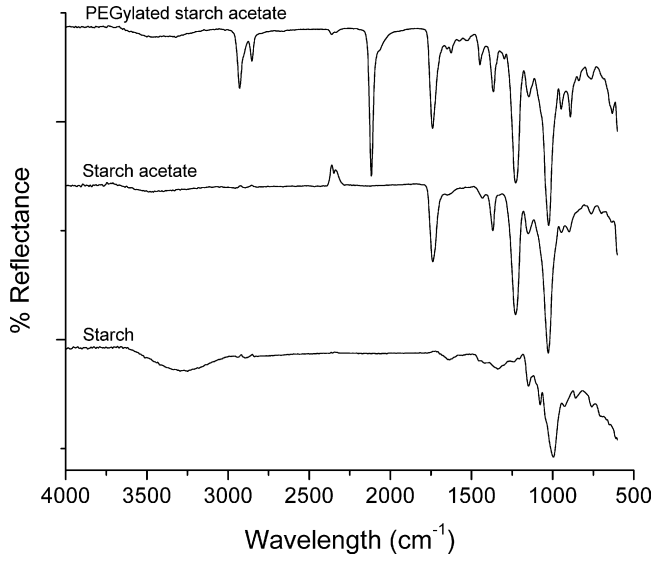

Fig. 2. FTIR spectra of starch, starch acetate and PEGylated starch acetate (SA-PEG1900).

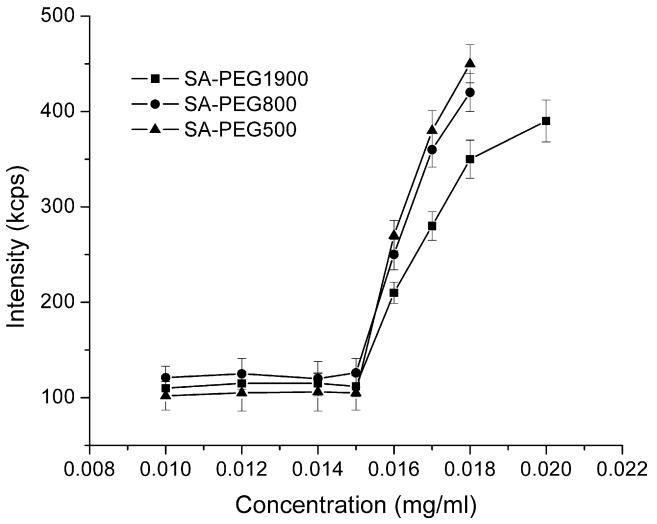

Fig. 3. Critical micelle concentration (CMC) of the PEGylated starch acetate nanoparticles.

respectively at 25 °C. Recently, self-aggregated nanoparticles have received much attention as a material for drug delivery systems since the drug incorporation can be achieved without degradation under harsh reaction conditions required for conjugation, and at the same time, the self-aggregates are eventually formed without a cross-linker. Polymeric self-assemblies are usually formed from block copolymers or hydrophobically modified water-soluble polymers. The ratio of the size between head group and 'tail' determines the solubility in aqueous solution and its aggregation behavior (hydrophobic effect). Therefore, by using PEG of different molecular weights, self-aggregates of different sizes or different shapes could be developed.

3.3. Zeta potential of PEGylated starch acetate nanoparticles

The nanoparticles formed from starch had a net negative charge with a mean zeta potential of −10.3 mV at neutral pH. The zeta potential of different samples at neutral pH (physiological pH) is provided in Table 2. Acetylation of starch made the nanoparticles highly negative, with zeta potential of −33.5 mV at neutral pH. However, conjugation with PEG1900 increased its zeta potential to a potential of −12.1 mV at neutral pH. The intestinal pH is usually 6–7; therefore, the PEG conjugated nanoparticles seem to be suitable for intestinal delivery. A low-negative zeta potential of these nanoparticles at neutral pH is sufficient to provide excellent stability and shelf life for a formulation prepared from it. Zeta potential has been suggested to play an important role in particle uptake because the surface of the intestinal mucosa is negatively charged owing to the presence of glycocalyx. Particles with a high positive surface charge like chitosan are usually attracted by the intestinal mucosa which helps in increasing the intestinal absorption of the encapsulated drug. However, the strong electrostatic interaction between the positively charged particles and the negatively charged glycocalix, may slow down the progression and penetration of these particles to the epithelial cell surface, reducing their uptake. Also, it has been shown that non-ionized particles have a greater affinity for M cells than for ionized particles (Jani, Halbert, Langridge & Florence, 1989) or positively charged particles (Shakweh, Ponchel & Fattal, 2004). Therefore, the low-negative potential of PEGylated starch acetate nanoparticles seems to be desirable from a particle uptake and drug absorption point of view.

Table 2
Particle size, zeta potential, % hemolysis, cytotoxicity and bio-adhesiveness (force maximum and work of adhesion) of PEGylated starch acetate nanoparticles.

	Average particle size (d nm)	Zeta potential at pH 7.4 (mV)	Hemolysis (%)	Cell viability (%)	F_{max} (mN)	W_{ad} (mN mm)
Chitosan	–	–	–	–	432 ± 34	144 ± 11
Starch	–	−10.3	–	–	–	–
Starch Acetate (SA)	–	−33.5	–	–	479 ± 112	179 ± 41
SA-PEG500	54 ± 5	−4.22	4.2 ± 0.5	8	1503 ± 126	556 ± 39
SA-PEG800	43 ± 3	−13.2	3.8 ± 0.4	9	1634 ± 145	571 ± 35
SA-PEG1900	32 ± 2	−12.1	0.2 ± 0.1	98	1708 ± 133	595 ± 42

3.4. Cytotoxicity of PEGylated starch acetate

L929 cell is an established cell line which has been extensively used for cytotoxicity studies. The percentage of viable cells compared with negative control represented the level of cytotoxicity of the particles. Percentage of viable cells on incubation of PEGylated starch acetate prepared with PEG 1900 (SA-PEG1900) was more than 98%, which confirms that they are non-toxic to the L-929 cells. However, the other two derivatives (SA-PEG500 and SA-PEG800) were toxic with a cell viability less than 10% (Table 2). Polyethylene glycol and its chemical derivatives are widely used as vehicles or co-solvents in many pharmaceutical compositions. However, PEG polymers of low molecular weight differ significantly from polymers of higher molecular weight in their physicochemical properties, biological effects on cell permeability and their absorption and excretion, as well as their higher toxicity and possibly genotoxicity. PEG of low molecular weight is more toxic than high molecular weight PEG (Campbell, 1984). It has been reported that low molecular weight PEG induces chromosome aberrations in Chinese hamster cells cultured *in vitro* (Biondi, Motta & Mosesso, 2002). There are several reports indicating potential nephrotoxicity in patients receiving continuous infusions of polyethylene glycol 400, used as a diluent in hospital intravenous preparations (Laine, Hossain, Solis & Adams, 1995) and in burn victims treated with topical polyethylene glycol-based creams (Bruns, Herold, Rodeheaver & Edlich, 1982). A red-blood-cell lysis experiment was done and reported in Table 2. Hemolysis caused by SA-PEG1900 was practically nil compared to the other two derivatives which were in the order of 4%. These results support the cytotoxicity results. Thus, the novel derivative developed from starch acetate and PEG1900 seems to be a better candidate for intestinal delivery, since it could be highly compatible with intestinal cell walls.

3.5. Mucoadhesiveness of PEGylated starch acetate nanoparticles

SA-PEG1900 nanoparticles were attached to the cylindrical probe using double sided adhesive tapes. This probe was immersed in the test medium for 10 min prior to attachment to a duodenal part of small intestinal mucosa. The probe was pulled out at a speed of 0.5 mm/s after attachment to the mucosa at a contact force of 0.05 N and contact time of 1 s. Table 2 shows the F_{max} of pre-hydrated nanoparticle discs of PEGylated nanoparticles, starch acetate and chitosan nanoparticles after attachment to duodenal mucosa. The results showed that the F_{max} of SA-PEG1900 was significantly higher than that of starch acetate and chitosan. Work of adhesion (W_{ad}) for PEGylated nanoparticles was also significantly higher at 595.7 mN mm than the 179.1 and 144.4 mN mm for starch acetate and chitosan respectively. The significant increase in bioadhesion for PEGylated nanoparticles could be because of chain "entanglements" between PEG and mucin chain and slow relaxation of mucin during surface seperation (Claesson, Blomberg, Froberg, Nylander & Arnebrant, 1995; Malmsten, Blomberg, Claesson, Carlstedt & Ljusegren, 1992).

3.6. Tight junction visualization

Tight junction visualization studies demonstrated that PEGylated starch acetate nanoparticles are capable of opening tight junctions. The control Caco-2 cells stained with rhodamine phalloidin, to visualize actin, showed uniform staining pattern as shown in Fig. 4(a). However, cells treated with PEGylated starch acetate nanoparticles displayed a disrupted staining pattern (Fig. 4(b)). Actin filaments were observed to be discontinuous and disrupted as evidenced from the staining pattern and the clumping. To further investigate the effect on the tight junction proteins, immunofluorescence studies using anti ZO-1 were done. ZO-1 is a tight junction associated protein which plays an important role in tight junction functional regulation. The effect of nanoparticles on ZO-1 tight junction proteins was evaluated on Caco 2 cell monolayers and is also shown in Fig. 4. The untreated cells were observed as smooth lines at the cell–cell junction (Fig. 4(c)); whereas, for PEGylated starch acetate nanoparticle-treated cells the staining intensity was weaker at cell–cell contact sites (Fig. 4(d)). Tight junctions are composed of transmembrane proteins occludin, claudins and junctional adhesion molecules which intercalate with corresponding proteins from adjacent cells to form the intercellular barrier. These proteins associate with peripheral membrane proteins, including the membrane proteins zonula occludens (ZO-1 to 3), which join the transmembrane proteins to the actin cytoskeleton. ZO-1 and Occludin phosphorylation are associated with stimulus-induced tight junction disassembly and paracellular permeability changes. In the untreated cells, ZO-1 was observed as smooth lines at cell–cell junctions. The immunofluorescent staining intensity of PEGylated starch acetate nanoparticle-treated cells were observed to be weaker, when compared to control which indicated the loss of ZO-1 from sites of cell–cell contact.

3.7. In vitro release of insulin from PEGylated starch acetate nanoparticles

The encapsulation efficiency of SA-PEG1900 was evaluated to be 83% and the drug loading to be 1.3 ± 0.1 IU/mg. In order to obtain some preliminary information about the potential use of PEGylated starch acetate as a protein delivery system for oral administration, *in vitro* hydrolysis studies were performed in simulated gastric (SGF, pH 1.2) and intestinal fluids (SIF, pH 6.8); and pH 7.4 phosphate buffered saline. A 20% release of insulin was observed in pH 1.2 and around 55% in pH 7.4 buffer during a period of 2 h as shown in Fig. 5. A moderate sustained release of insulin was observed at pH 6.8 and 7.4, with 60% and 80% release of insulin in 8 h of study. The gastric retention time of particles is considered to be 1–2 h, hence the 20% release in gastric environment can be considered comparatively low. The release of insulin was controlled by diffusion or by swelling followed by diffusion and stabilizes insulin preventing its self-association. Increase in cellular permeability and improved bioavailability of orally administered protein drugs

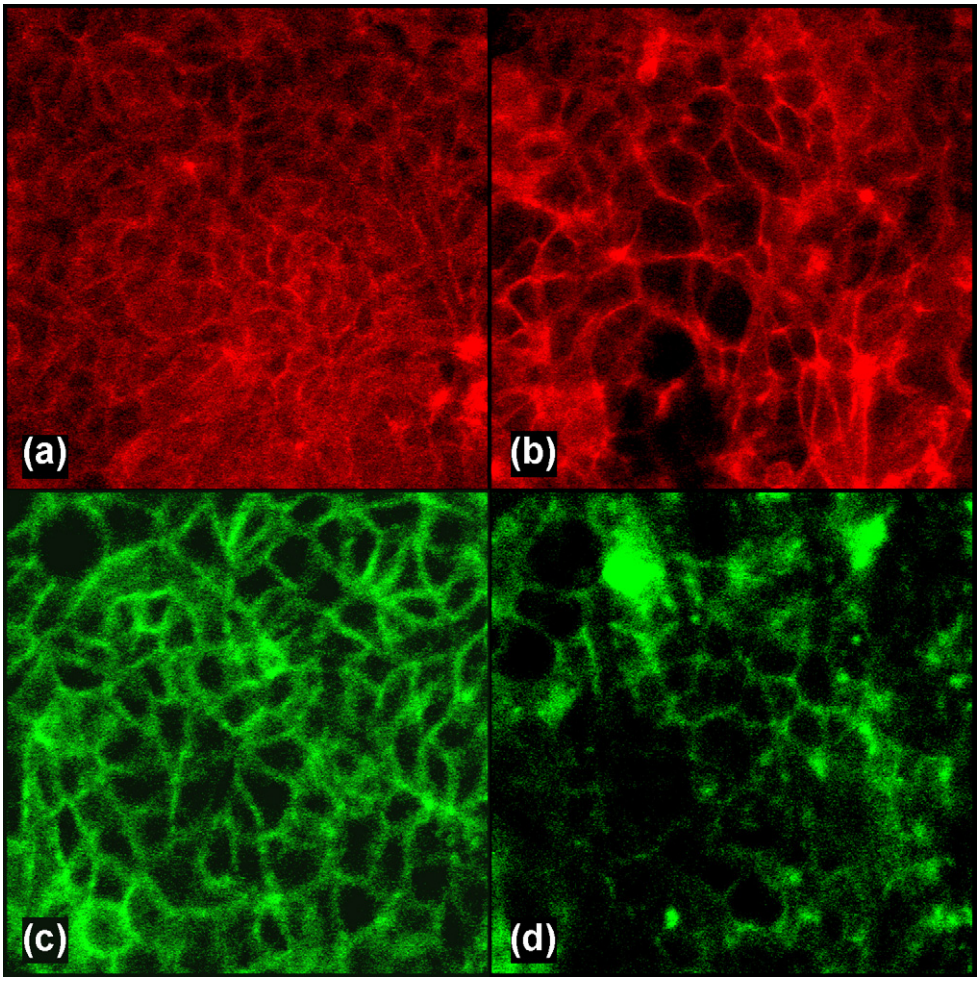

Fig. 4. Confocal images (20×) of Caco 2 cell – actin. (a) Caco cells without any treatment (control). (b) Caco cells exposed to 5 mg of SA-PEG1900 nanoparticles for 1 h – tight-junction protein ZO-1. (c) Caco cells without any treatment (control). (d) Caco cells exposed to 5 mg of SA-PEG1900 nanoparticles for 1 h.

has been reported with several polymeric derivatives. Therefore, SA-PEG1900 nanoparticles are also expected to increase the bioavailability of insulin. However, this needs to be studied on diabetic animals.

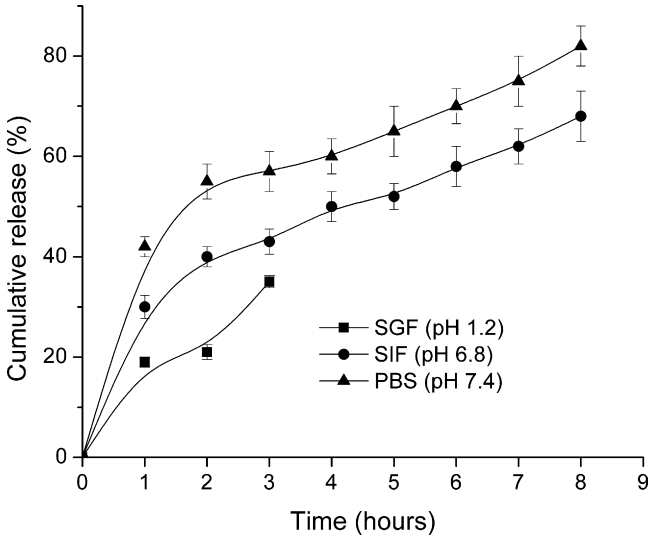

Fig. 5. *In vitro* release profile of insulin from nanoparticles of SA-PEG1900 in SGF (pH 1.2), SIF (pH 6.8) and phosphate buffered saline (pH 7.4).

3.8. Conformation of released insulin

CD spectra provide both qualitative and quantitative information about protein conformations (Holzwarth & Doty, 1965). The CD spectra of insulin gave a negative band, which is based on the anti-parallel beta structure of insulin, due to the dimer form while the negative peak at 208 nm is assigned to its α-helical structure (Prieto, Wilmans, Jimenez, Rico & Serrano, 1997). The far-UV CD spectra of insulin released from the formulation at pH 6.8 were recorded. At near neutral pH, the far-UV CD spectra revealed no significant differences in the secondary structure of the released insulin as compared to the native insulin. The corresponding CD deconvolution and predicted secondary structure (SELCON method) is given in Table 3. CD and spectral deconvolution analysis demonstrate substantial retention of native α-helix content. Insulin fibrillation may be enhanced by partial unfolding of the monomer by a variety of perturbations including solvents used for coating and the interaction between hydrophobic surfaces and accelerated

Table 3
CD Deconvolution and predicted secondary structure of insulin released from PEGylated starch acetate nanoparticles.

Sample	Fractional composition (%)			
	(-helix	(-strand	Turns	Random
Native insulin	35 ± 2	12 ± 1	22 ± 2	31 ± 2
Released insulin	36 ± 2	12 ± 1	23 ± 2	31 ± 2

under acidic conditions (Ahmad, Millett, Doniach, Uversky & Fink, 2003; Nielsen et al., 2001). However, at near neutral pH, the far-UV CD spectra revealed no significant differences in the secondary structure of the released insulin as compared to the native insulin.

4. Conclusion

Biodegradable polymers are typically used to control the rate of drug release from parenteral drug delivery systems. Such polymers hold enormous potential, especially for the delivery of peptides and proteins. Biodegradable polymers, such as starch, have been extensively studied for pharmaceutical applications. The present investigation highlighted the prospect of using PEGylated starch acetate nanoparticles for controlled drug delivery utilizing its self aggregation property. Micellar nanoparticles are formed on self association of PEGylated starch acetate in the presence of aqueous insulin solution. The hydrophobic core of starch acetate protects insulin from the gastric environment. It has been demonstrated that the insulin released from these nanoparticles was stable with no conformational changes. It has been reported that polymeric nanoparticles exhibited a size dependent uptake from the intestine (Jani, Halbert, Langridge & Florence, 1990; Shakweh, Calvo, Gouritin, Alphandary & Fattal, 2002). Particles less than 100 nm showed a significant absorption with no absorption of particles larger than 300 nm. The size dependency was proportional to the extent of the glucose level reduction when such insulin-loaded polymeric particles were administered orally (Desai, Labhasetwar, Amidon & Levy, 1996; Lamprecht, Schafer & Lehr, 2001; Yan, Jun-Min, Hui-Ying, Ying-Jian, Hui & Gang, 2002). The hypoglycemic effect was prolonged for 100 nm particles, because these particles got absorbed more compared to larger particles. Therefore, it could be assumed that the smaller size of the SA-PEG1900 nanoparticles significantly helps in their possible uptake by the intestinal mucosa and possible prolonged hypoglycemic effect. The non-cytotoxic nature of the SA-PEG1900 nanoparticles has been established through the MTT assay. Polyethylene glycol is known to be non-cytotoxic. Therefore, conjugation of polyethylene glycol with starch acetate to form self aggregates does not affect the non-cytotoxic nature of the particles. These self-aggregated nanoparticles could be utilized as an excellent carrier for the intestinal delivery of insulin. Release of insulin within 2 h was only less than 20%. And also the bioadhsiveness of the nanoparticles formed was significantly higher than that of chitosan. The present study indicates that PEG modified starch acetate is a good approach for controlled delivery of insulin or other proteins for various therapeutic applications.

Acknowledgement

We are grateful to the Director and the Head BMT Wing of SCTIMST for providing facilities for the completion of this work. This work was supported by the Department of Science & Technology, Govt. of India through the project 'Facility for nano/microparticle based biomaterials – advanced drug delivery systems' #8013, under the Drugs & Pharmaceuticals Research Programme.

References

Ahmad, A., Millett, I. S., Doniach, S., Uversky, V. N., & Fink, A. L. (2003). Partially folded intermediates in insulin fibrillation. *Biochemistry*, *42*(39), 11404–11416.

Biondi, O., Motta, S., & Mosesso, P. (2002). Low molecular weight polyethylene glycol induces chromosome aberrations in Chinese hamster cells cultured in vitro. *Mutagenesis*, *17*(3), 261–264.

Bruns, D. E., Herold, D. A., Rodeheaver, G. T., & Edlich, R. F. (1982). Polyethylene glycol intoxication in burn patients. *Burns, Including Thermal Injury*, *9*(1), 49–52.

Campbell, A. M. (1984). Fusion procedures. In A. M. Campbell (Ed.), *Monoclonal Antibody Technology* (pp. 120–134). Amsterdam: Elsevier Science Publishers.

Chiou, S. H., & Wu, W. T. (2004). Immobilization of Candida rugosa lipase on chitosan with activation of the hydroxyl groups. *Biomaterials*, *25*(2), 197–204.

Claesson, P. M., Blomberg, E., Froberg, J. C., Nylander, T., & Arnebrant, T. (1995). Protein interactions at solid-surfaces. *Advances in Colloid and Interface Science*, *57*, 161–227.

Couillet, I., Hughes, T., & Maitland, F. (2005). Synergistic effects in aqueous solutions of mixed wormlike micelles and hydrophobically modified polymers. *Macromolecules*, *38*(12), 5271–5282.

Daoud-Mahammed, S., Ringard-Lefebvre, C., Razzouq, N., Rosilio, V., Gillet, B., Couvreur, P., et al. (2007). Spontaneous association of hydrophobized dextran and poly-beta-cyclodextrin into nanoassemblies. Formation and interaction with a hydrophobic drug. *Journal of Colloid and Interface Science*, *307*(1), 83–93.

Desai, M. P., Labhasetwar, V., Amidon, G. L., & Levy, R. J. (1996). Gastrointestinal uptake of biodegradable microparticles: Effect of particle size. *Pharmaceutical Research*, *13*(12), 1838–1845.

Guan, J., & Hanna, M. A. (2004). Extruding foams from corn starch acetate and native corn starch. *Biomacromolecules*, *5*(6), 2329–2339.

Holzwarth, G., & Doty, P. (1965). The ultraviolet circular dichroism of polypeptides. *Journal of the American Chemical Society*, *87*, 218–228.

Hussain, N., Jaitley, V., & Florence, A. T. (2001). Recent advances in the understanding of uptake of microparticulates across the gastrointestinal lymphatics. *Advanced Drug Delivery Reviews*, *50*(1/2), 107–142.

Jani, P., Halbert, G. W., Langridge, J., & Florence, A. T. (1989). The uptake and translocation of latex nanospheres and microspheres after oral administration to rats. *Journal of Pharmacy and Pharmacology*, *41*(12), 809–812.

Jani, P., Halbert, G. W., Langridge, J., & Florence, A. T. (1990). Nanoparticle uptake by the rat gastrointestinal mucosa: Quantitation and particle size dependency. *Journal of Pharmacy and Pharmacology*, *42*(12), 821–826.

Kim, J. E., Cha, E. J., & Ahn, C. H. (2010). Reduction-sensitive self-aggregates as a novel delivery system. *Macromolecular Chemistry and Physics*, *211*(8), 956–961.

Kitchens, K. M., Kolhatkar, R. B., Swaan, P. W., Eddington, N. D., & Ghandehari, H. (2006). Transport of poly(amidoamine) dendrimers across Caco-2 cell monolayers: Influence of size, charge and fluorescent labeling. *Pharmaceutical Research*, *23*(12), 2818–2826.

Korhonen, O., Kanerva, H., Vidgren, M., Urtti, A., & Ketolainen, J. (2004). Evaluation of novel starch acetate-diltiazem controlled release tablets in healthy human volunteers. *Journal of Controlled Release*, *95*(3), 515–520.

Laine, G. A., Hossain, S. M., Solis, R. T., & Adams, S. C. (1995). Polyethylene glycol nephrotoxicity secondary to prolonged high-dose intravenous lorazepam. *Annals of Pharmacotherapy*, *29*(11), 1110–1114.

Lamprecht, A., Schafer, U., & Lehr, C. M. (2001). Size-dependent bioadhesion of micro- and nanoparticulate carriers to the inflamed colonic mucosa. *Pharmaceutical Research*, *18*(6), 788–793.

Malmsten, M., Blomberg, E., Claesson, P., Carlstedt, I., & Ljusegren, I. (1992). Mucin layers on hydrophobic surfaces studied with ellipsometry and surface force measurements. *Journal of Colloid and Interface Science*, *151*(2), 579–590.

Michailova, V., Titeva, S., Kotsilkova, R., Krusteva, E., & Minkov, E. (2001). Influence of hydrogel structure on the processes of water penetration and drug release from mixed hydroxypropylmethyl cellulose/thermally pregelatinized waxy maize starch hydrophilic matrices. *International Journal of Pharmaceutics*, *222*(1), 7–17.

Mosmann, T. (1983). Rapid colorimetric assay for cellular growth and survival: Application to proliferation and cytotoxicity assays. *Journal of Immunological Methods*, *65*(1-2), 55–63.

Nagarajan, R. (2011). Amphiphilic surfactants and amphiphilic polymers: Principles of molecular assembly. In R. Nagarajan (Ed.), *Amphiphiles: Molecular assembly and applications, acs symposium series* (pp. 1–22). Washington DC: American Chemical Society.

Nielsen, L., Khurana, R., Coats, A., Frokjaer, S., Brange, J., Vyas, S., et al. (2001). Effect of environmental factors on the kinetics of insulin fibril formation: Elucidation of the molecular mechanism. *Biochemistry*, *40*(20), 6036–6046.

Nilsson, S., Thuresson, K., Lindman, B., & Nyström, B. (2000). Associations in mixtures of hydrophobically modified polymer and surfactant in dilute and semidilute aqueous solutions. A rheology and PFG NMR self-diffusion investigation. *Macromolecules*, *33*, 9641–9649.

Nutan, M. T., Soliman, M. S., Taha, E. I., & Khan, M. A. (2005). Optimization and characterization of controlled release multi-particulate beads coated with starch acetate. *International Journal of Pharmaceutics*, *294*(1-2), 89–101.

Nutan, M. T., Vaithiyalingam, S. R., & Khan, M. A. (2007). Controlled release multiparticulate beads coated with starch acetate: Material characterization, and identification of critical formulation and process variables. *Pharmaceutical Development and Technology*, *12*(3), 307–320.

Ogura, T. (2004). Modified starch and utilization. In F. Hidetsugu, T. Komaki, S. Hizukuri, & K. Kainuma (Eds.), *Encyclopedia on Starch Science* (pp. 393–427). Tokyo: Asakura-shoten.

Organisation, I. S. (2009). Biological evaluation of medical devices Part 5: Tests for in vitro cytotoxicity: International Standards Organisation.

Pajander, J., Soikkeli, A. M., Korhonen, O., Forbes, R. T., & Ketolainen, J. (2008). Drug release phenomena within a hydrophobic starch acetate matrix: FTIR mapping of tablets after in vitro dissolution testing. *Journal of Pharmaceutical Sciences*, *97*(8), 3367–3378.

Pisárčik, M., Devínsky, F., & Švajdlenka, E. (1996). Spherical dodecyltrimethylammonium bromide micelles in the limit region of transition to rod-like micelles. A light scattering study. *Colloids and Surfaces A: Physicochemical and Engineering Aspects*, *119*(2–3), 115–122.

Pohja, S., Suihko, E., Vidgren, M., Paronen, P., & Ketolainen, J. (2004). Starch acetate as a tablet matrix for sustained drug release. *Journal of Controlled Release*, *94*(2-3), 293–302.

Prieto, J., Wilmans, M., Jimenez, M. A., Rico, M., & Serrano, L. (1997). Non-native local interactions in protein folding and stability: Introducing a helical tendency in the all beta-sheet alpha-spectrin SH3 domain. *Journal of Molecular Biology*, *268*(4), 760–778.

Pu, H., Chen, L., Li, X., Xie, F., Yu, L., & Li, L. (2011). An oral colon-targeting controlled release system based on resistant starch acetate: Synthetization, characterization, and preparation of film-coating pellets. *Journal of Agricultural and Food Chemistry*, *59*(10), 5738–5745.

Rangelov, S., Petrov, P., Berlinova, I., & Tsvetanov, C. (2004). Association properties of a high molecular weight poly(propylene oxide–b–ethylene oxide) diblock copolymer in aqueous solution. *Polymer Bulletin*, *52*, 155–161.

Reddy, N., & Yang, Y. (2009). Preparation and properties of starch acetate fibers for potential tissue engineering applications. *Biotechnology and Bioengineering*, *103*(5), 1016–1022.

Shakweh, M., Calvo, P., Gouritin, B., Alphandary, H., & Fattal, E. (2002). Uptake of biodegradable nano and microparticles by Peyer's patches after oral administration to mice. 4th World meeting on pharmaceutics, biopharmaceutics and pharmaceutical technology: Florence, 8–11 April 2002: proceedings. France: Châtenay-Malabry.

Shakweh, M., Ponchel, G., & Fattal, E. (2004). Particle uptake by Peyer's patches: A pathway for drug and vaccine delivery. *Expert Opinion on Drug Delivery*, *1*(1), 141–163.

Sreerama, N., Venyaminov, S. Y., & Woody, R. W. (1999). Estimation of the number of alpha-helical and beta-strand segments in proteins using circular dichroism spectroscopy. *Protein Science*, *8*(2), 370–380.

Sreerama, N., & Woody, R. W. (2000). Estimation of protein secondary structure from circular dichroism spectra: Comparison of CONTIN, SELCON, and CDSSTR methods with an expanded reference set. *Analytical Biochemistry*, *287*(2), 252–260.

Tuovinen, L., Peltonen, S., Liikola, M., Hotakainen, M., Lahtela-Kakkonen, M., Poso, A., et al. (2004). Drug release from starch-acetate microparticles and films with and without incorporated alpha-amylase. *Biomaterials*, *25*(18), 4355–4362.

Tuovinen, L., Ruhanen, E., Kinnarinen, T., Ronkko, S., Pelkonen, J., Urtti, A., et al. (2004). Starch acetate microparticles for drug delivery into retinal pigment epithelium-in vitro study. *Journal of Controlled Release*, *98*(3), 407–413.

United States Pharmacopeial Convention, I. (2005). The United States Pharmacopeia. USP 28 pp. 2855-2858). Rockville, MD, USA.

van Veen, B., Pajander, J., Zuurman, K., Lappalainen, R., Poso, A., Frijlink, H. W., et al. (2005). The effect of powder blend and tablet structure on drug release mechanisms of hydrophobic starch acetate matrix tablets. *European Journal of Pharmaceutics and Biopharmaceutics*, *61*(3), 149–157.

Wintgens, V., & Amiel, C. (2005). Surface plasmon resonance study of the interaction of a beta-cyclodextrin polymer and hydrophobically modified poly(N-isopropylacrylamide). *Langmuir*, *21*(24), 11455–11461.

Xu, W., Yang, W., & Yang, Y. (2009). Electrospun starch acetate nanofibers: Development, properties, and potential application in drug delivery. *Biotechnology Progress*, *25*(6), 1788–1795.

Xu, Y., Miladinov, V., & Hanna, M. A. (2004). Synthesis and characterization of starch acetates with high substitution. *Cereal Chemistry*, *81*(6), 735–740.

Yan, P., Jun-Min, Z., Hui-Ying, Z., Ying-Jian, L., Hui, X., & Gang, W. (2002). Relationship between drug effects and particle size of insulin-loaded bioadhesive microspheres. *Acta Pharmacologica Sinica*, *23*, 1051–1056.